Journal of Statistical Physics, Vol. 67, Nos. 3/4, 1992

Finite-Size Scaling Study of a First-Order Temperature-Driven Symmetry-Breaking Structural Phase Transition

J. R. Morris[1] and R. J. Gooding[2]

Received October 23, 1991; final January 7, 1992

We present a study of finite-size effects in a model exhibiting a first-order temperature-driven symmetry-breaking structural phase transition in the $L_\perp \times \infty$ cylindrical geometry in the $L_\perp \to \infty$ limit. Exact studies demonstrate the applicability of our scaling ansatz even in the one-dimensional limit, making this model ideal for studying finite-size effects. The scaling ansatz, similar to the previously developed ansatz for field-driven transitions, demonstrates that latent heat is crucial in driving these transitions. This ansatz is supported by a 2×2 phenomenological transfer matrix based upon the symmetries of the system; this produces an analytic free energy which has the scaling form. Order parameter probability distributions show that the high- and low-temperature phases coexist only in a small finite-size-affected regime near the bulk transition temperature; this regime vanishes exponentially fast as $L_\perp$ diverges.

KEY WORDS: First-order transitions; finite-size effects; coexistence; structural phase transition.

1. INTRODUCTION

Since the origins of statistical mechanics, one of the major goals has been the understanding of phase transitions. Much progress has been made, especially for second-order transitions: the successes start with Onsager's exact solution of the Ising model,[1] and include the developments made by scaling theories of critical phenomena, the idea of universality, and the subsequent renormalization group concepts and techniques.

[1] Laboratory of Atomic and Solid State Physics, Cornell University, Ithaca, New York 14853-2501.

[2] Department of Physics, Queen's University, Kingston, Ontario, Canada K7L 3N6.

0022-4715/92/0500-0471$06.50/0

The progress in the field of first-order transitions has not been as complete. It has been established that a first-order transition is characterized by an essential singularity in the free energy.[2] The only two exactly solved models with first-order transitions, the mean-field model and the wetting model of ref. 3, do not have such a singularity due to the incorrect account (mean-field) or absence (wetting model) of the appropriate droplet configurations. This singularity only occurs in the thermodynamic limit—for a finite-size system, the transition is "rounded" such that the free energy is analytic; this rounding regime vanishes as the system size diverges.[4-7],[3] The exactly solvable model[3] demonstrates identical behavior. Due to the fact that the effects of the finite system are predominant only in a narrow region near the transition, we choose to refer to this as the "finite-size-affected" regime.

It has been suggested[2] that because a system undergoing a first-order phase transition is characterized by an essential singularity, important physical consequences result. In equilibrium, the system will have no indications of the incipient phase, viz. there are no thermodynamically stable "precursors" to the transition. Simply phrased, coexistence occurs only at the transition. At all other temperatures, evidence of coexistence is an indication that the system is not in true equilibrium. For finite systems, however, a form of coexistence may in principle be observed over a small but finite region. This has been previously demonstrated for hypercubic systems.[5]

Our primary interest is in first-order temperature-driven symmetry-breaking transitions, viz. those relevant to structural phase transitions.[8] Although there are some exact results known for the Potts model,[9-11] there is no fully solved model with a symmetry-breaking transition exhibiting a first-order transition. The model we present[12,13] has the remarkable property (for the appropriate choice of parameters) that the exact thermodynamics of the system exhibits scaling properties (defined below) even in the limit of one dimension. This model utilizes vibrational entropy in determining the characteristics of the finite-size scaling regime: essentially, one parameter of the model allows us to adjust the bulk entropy change at the transition. The important finite-size features of symmetry-breaking transitions may be understood by examining only two of the eigenvalues of the associated transfer matrix, as we shall elucidate below; this model is ideal for demonstrating this behavior, due to the simplicity of the model (only two low-temperaature variants) and the rapid crossover to the bulk limit.

[3] See ref. 6 for review articles on finite-size scaling.

We begin by reviewing the arguments leading to the well-estabished[4,7] finite-size scaling ansatz for field-driven transitions, appropriate for systems such as the Ising model at fixed temperature $T < T_c$, and extend these arguments to develop a similar ansatz for the case of temperature-driven symmetry-breaking transitions. The forms of the scaling equations are developed specifically for $L_\perp^{d-1} \times \infty$ systems, which may be studied using the transfer matrix (TM) formalism. In comparison with the field-driven case, an additional length scale is now necessary for the symmetry-breaking case, associated with spacings of the domain walls between high- and low-temperature phases. This length diverges at the transition as $L_\perp \to \infty$, while leaving the bulk correlation length finite. The finite-size scaling ansatz is valid in a "scaling regime" where $L_\perp$ is large enough that the properties of the finite system approach the limit of the bulk properties. In this regime, the finite-size-affected region (near the transition temperature T_t, where the effects are most important) is small, and in general vanishes exponentially fast as $L_\perp$ diverges.[7] Our ansatz predicts the width of this regime; for the temperature-driven case, the entropy change that occurs at the transition plays an *essential* role in defining this width.

In Section 3 we present our model, one which controls the vibrational entropy in both the high- and low-temperature phases to allow for the direct study of the finite-size effects for symmetry-breaking transitions. Using a phenomenological reduction of the TM, we show that three of the eigenvalues are relevant to the transition (one for the high-temperature phase and two for the low-temperature variants), but that the important features of the finite-size rounding may be understood by examination of only two of the values: namely, the dominant eigenvalue λ_0 and also the *smallest* of the eigenvalues that approach λ_0 as $L_\perp$ diverges. Alternatively, the scaling is controlled by the shortest of the diverging lengths of the system. This phenomenological TM is similar to that proposed for transitions that do not exhibit symmetry breaking.[3,7,14]

Numerical results presented in Section 4 demonstrate that the finite-size scaling ansatz and the phenomenological reduction of the TM describe the exact results found for our model. We examine two versions of our system: in one case, the local order parameter may take on only five discrete values; second, we examine the case where the local order parameter is a continuous scalar variable. In the latter case, the remarkable scaling behavior for small $L_\perp$ is shown to be due to the change in the entropy associated with small-amplitude displacements, i.e., the vibrational entropy. The discrete version lacks these excitations, and thus has a smaller change of entropy; therefore the thermodynamic quantities show a considerably slower approach to the scaling regime. Numerical results for these cases

show that the finite-size scaling regime is well defined; within this temperature range the model shows evidence of coexistence. As $L_\perp$ increases, the entropy and the mean-squared order parameter become scaling functions, confirming the predictions of the finite-size scaling ansatz.

Lastly, an analytic approach to the one-dimensional limit of our model demonstrates that anharmonic couplings incorporated in the model are essential for the remarkable scaling behavior. The transfer-integral (TI) problem for this model is transformed into the form of a Schrödinger equation; the "ground-state energy" of this pseudo-Schrödinger equation is directly related to the free energy of the 1D system. This pseudo-Schrödinger equation is appropriate in the "displacive" limit,[15] where the local order parameter varies slowly between lattice sites. Near the temperature T_1, the WKB approximation allows for a direct prediction of the gap at the near crossing of levels. Using this, we directly show the effect of the anharmonic coupling on the gap in the spectrum, thus conclusively demonstrating how the coupling generates a system with a vanishingly small finite-size-affected regime even for $L_\perp = 1$. Further, at low temperatures a WKB approximation for the splitting between the energies of the ground state and the first excited state allows for a direct evaluation of the importance of domain walls on the thermodynamics of the finite-size systems. The correction to the free energy due to the splitting caused by domain walls is *extremely* small; quasiharmonic corrections are significantly more important.[16]

2. FINITE-SIZE SCALING ANSATZ FOR FIRST-ORDER TEMPERATURE-DRIVEN TRANSITIONS WITH CYLINDRICAL GEOMETRY

We begin by reviewing the finite-size scaling hypothesis appropriate for temperature-driven, first-order transitions. The arguments for this ansatz follow by analogy from those presented for field-driven transitions[7]; we present both since the comparison to the well-developed field-driven case allows for the straightforward development of the temperature-driven finite-size scaling ansatz.

The system size is taken to be $L_{||} \times L_\perp^{d-1}$; we are interested in the limit that $L_{||}$ is longer than all other length scales in the system. Furthermore, periodic boundary conditions are enforced in all directions. This assumption of cylindrical geometry is appropriate for the results of strip TM studies.

In the limit $L_{||} \to \infty$, there is no transition if $L_\perp$ is finite. For sufficiently large $L_\perp$, however, we expect that the system will have properties approaching those of the bulk ($L_\perp \to \infty$) limit except in a narrow regime

near the first-order transition temperature T_1, viz. the finite-size-affected regime. When $L_\perp$ is finite and $T < T_1$, the system is mainly composed of domains of the symmetry-broken phases; in equilibrium there are no macroscopically occupied regions of the high-temperature phase at temperatures well below T_1 (see Fig. 1a). This will be demonstrated for our model in Section 4, and is consistent with the fact that coexistence only occurs in equilibrium exactly at the transition temperature. The domain walls form surfaces roughly perpendicular to the long direction ($L_{||}$), and destroy long-range order for the finite-size system. We denote the characteristic spacing of these domain walls by ξ_1, in anticipation of the notation in Section 3. This length is important to the scaling properties of the system, and may be calculated using the TM formalism. General arguments[7,17] show that

$$\xi_1(L_\perp) \sim \exp(\sigma L_\perp^{d-1}), \qquad \sigma \equiv \beta \Sigma(T, L_\perp) \tag{1}$$

where $\Sigma(T, L_\perp)$ is the appropriate domain-wall free energy density,[7,17] and is a function of field and/or temperature. It is believed that[7,18]

$$\Sigma(L_\perp) - \Sigma_\infty \approx \frac{w}{L_\perp^{d-1}} \ln L_\perp$$

and thus one writes

$$\xi_1 \sim L_\perp^w \exp(\sigma_\infty L_\perp^{d-1}) \tag{2}$$

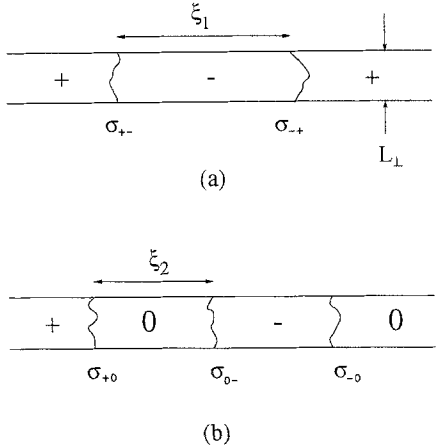

Fig. 1. Schematic structure of domains of $L_\perp \times \infty$ system (a) for $T < T_1$ and (b) for $T \approx T_1$. The symbols + and − indicate broken symmetry states, and 0 indicates the high-temperature phase. The values σ_{+-}, σ_{+0}, etc., indicate the appropriate reduced domain-wall free energy.

where Σ_∞ and σ_∞ are found from the $L_\perp \to \infty$ limit. Note that this length diverges *exponentially fast* with $L_\perp$.

All of this is similar to the field-driven case, where the transition must occur at $H=0$ due to the symmetry of the Hamiltonian about $H \to -H$. The length ξ_1 is a maximum at zero field for fixed $T < T_c$. The exponent w depends upon the boundary conditions in the perpendicular directions: for the field-driven first-order transition in the Ising model below T_c, exact results[7] demonstrate $w = 1/2$ for periodic boundary conditions and $w = 0$ for free boundary conditions.

For first-order symmetry-breaking transitions an additional length scale is important near the bulk transition temperature, which we now motivate. In our model, we shall consider the *simplest* case, i.e., there are *only* two low-temperature variants related by the symmetries of the Hamiltonian. The thermodynamic quantities do not show sharp, singular behavior, but instead show rounded behavior for a narrow range of temperatures near the transition. In this finite-size-affected regime, the system will be divided predominantly into domains of low- and high-temperature phases, with domain walls formed along $(d-1)$-dimensional surfaces perpendicular to the long $L_{||}$ direction (see Fig. 1b). We denote the characteristic spacing of these walls by ξ_2; this is the second important length scale. For $L_\perp$ finite we *define* the temperature $T_1(L_\perp)$ to be the temperature at which ξ_2 is a maximum. As in Eq. (2), this length is governed by the appropriate domain-wall free energy, and diverges exponentially with $L_\perp$. The domain wall spacings satisfy $\xi_1 > \xi_2$ for finite $L_\perp$. As will be demonstrated later, it is the length ξ_2 (or, more generally, the shortest of the diverging length scales) that is most important in understanding the finite-size-affected regime near T_1. Note also that, unlike ξ_1, ξ_2 diverges as $L_\perp \to \infty$ only at a unique temperature $T = T_1(L_\perp)$, which converges to the transition temperature. In the $L_\perp \to \infty$ limit, ξ_1 is infinite for all $T \leqslant T_1$ due to the twofold degeneracy of the low-temperature phase.

With this introduction, we are prepared to present the formulation of the finite-size scaling ansatz. We develop the temperature-driven case by comparison with the well-established field-driven case.[7,17] For the field-driven case, the singular part of the reduced Gibb's free energy density may be expressed as

$$g_s(H; L_\perp, L_{||}) \equiv \frac{G_s}{TV} = \frac{A}{V} \tilde{W}_H \left[B(T)\, h L_\perp^{d-1} \xi_1, \frac{L_{||}}{\xi_1} \right], \qquad h \equiv \frac{H}{T} \tag{3}$$

where the volume is $V = L_{||} L_\perp^{d-1}$ and G_s is the singular part of the total free energy. The scaling function $\tilde{W}_H(y, L_{||}/\xi_1)$ is universal, and $B(T)$ and A are nonuniversal amplitudes; A is assumed to be temperature inde-

pendent. Since g_s is intensive in the infinite-volume limit, $\tilde{W}_H(y, L_{||}/\xi_1)$ must be linear with $L_{||}/\xi_1$ as $L_{||}$ diverges. Then, the free energy becomes

$$g_s(H; L_\perp) = \frac{A}{L_\perp^{d-1}\xi_1} W_H[B(T)\, hL_\perp^{d-1}\xi_1] \tag{4}$$

In a similar fashion, for the temperature-driven case the free energy is of the form

$$g_s(T; L_\perp) = \frac{A}{L_\perp^{d-1}\xi_2} W_T[B(T)\, tL_\perp^{d-1}\xi_2] \tag{5}$$

where the reduced temperature t (viz., what drives the transition) is defined to be

$$t \equiv \frac{T - T_1(L_\perp)}{T_1(L_\perp)} \tag{6}$$

Note that the scaling combinations given in Eqs. (4) and (5) contain the characteristic volume $L_\perp^{d-1}\xi_2$ instead of the volume of the system; this is due to the fact that we are letting $L_{||}$, and therefore the total volume, tend to infinity. We anticipate that the size of single-phase domains will be on the order of this characteristic volume near the transition.

We now express the parameter $B(T)$ in terms of physical quantities by relating the above scaling form to the appropriate susceptibilities. We expect that g_s is a local maximum at the transition. Then, for the field-driven transition, the susceptibility at $h = 0$ is

$$\chi \equiv -\frac{1}{V}\left(\frac{\partial^2 G_s}{\partial H^2}\right)_{H=0} = -\frac{A}{T} L_\perp^{d-1}\xi_1 B^2(T)\, W_H''(0) \tag{7}$$

Note that the susceptibility may also be written in terms of spin–spin correlations as

$$\chi = \frac{1}{VT}\sum_{ij} (\langle s_i s_j\rangle - \langle s_i\rangle\langle s_j\rangle) \tag{8}$$

Let us make the crude approximation that particles are correlated over a length ξ_1 along the long direction, and are fully correlated perpendicular to this direction. We then assume that within a volume $L_\perp^{d-1}\xi_1$ the fluctuations are related to the spontaneous magnetization $m_0(T)$ by

$$\langle s_i s_j\rangle - \langle s_i\rangle\langle s_j\rangle \approx m_0^2(T) \tag{9}$$

and that outside of this volume the correlations are negligible. Using translational invariance, we can write the susceptibility as

$$\chi = \frac{m_0^2(T)}{T} L_\perp^{d-1} \xi_1 \tag{10}$$

which leads to the desired identification

$$B^2(T) = -\frac{m_0^2(T)}{A W_H''(0)} \tag{11}$$

In the case of the temperature-driven transition, the relevant susceptibility is the specific heat. At $T = T_1$, this is defined as

$$c_v(T_1) = -\frac{T_1}{V}\left(\frac{\partial^2 G}{\partial T^2}\right) = -A L_\perp^{d-1} \xi_2 B^2(T)\, W_T''(0) \tag{12}$$

In terms of the energy fluctuations this quantity is given by

$$c_v = \frac{1}{VT^2} \sum_{ij} (\delta E_i\, \delta E_j) \tag{13}$$

where $\delta E_i = E_i - \langle E_i \rangle$ is the deviation of the energy of particle i from the average energy per particle. We assume that the fluctuations in energy are on the order of the bulk ordering energy for correlated sites (within a volume $L_\perp^{d-1} \xi_2$), and zero otherwise:

$$\langle \delta E_i\, \delta E_j \rangle \approx l^2 \tag{14}$$

Here, l is the bulk latent heat per particle. These arguments yield

$$c_v(T_1) = L_\perp^{d-1} \xi_2 \frac{l^2}{T_1^2} \tag{15}$$

Comparison with the scaling form of the heat capacity then gives

$$B^2(T) = -\frac{(\Delta S)^2}{A W_T''(0)} \tag{16}$$

where $\Delta S = l/T_1(L_\perp)$ converges to the change of entropy per particle at the transition as $L_\perp \to \infty$.

These results combine to produce the well-known scaling ansatz[7]

$$g_s = \frac{A}{L_\perp^{d-1} \xi_1} W_H(y_h), \qquad y_h \equiv h m_0(T)\, L_\perp^{d-1} \xi_1 \tag{17a}$$

for the field-driven case. Similarly, for the temperature-driven transitions, the above results lead us to the finite-size scaling ansatz

$$g_s = \frac{A}{L_\perp^{d-1}\xi_2} W_T(y_t), \qquad y_t \equiv t\,\Delta S\, L_\perp^{d-1}\xi_2 \tag{17b}$$

Note that the scaling variables y_h and y_t incorporate the intuitive combination of the ratio of the bulk ordering energy (viz., the driving energy per particle times the characteristic domain size) to the thermal energy T. It is these combinations that determine the range in which finite-size effects are significant, viz., the finite-size-affected regime.

The scaling variable y_t provides an estimate for the width of this regime near the transition temperature T_1. For $|y_t| \to \infty$ we expect $W_T(y_t) \sim |y_t|$. Rounding is to be expected in a regime determined by $y_t \sim 1$, as discussed in ref. 7. From Eq. (17b) this defines the temperature range

$$\Delta T \sim \frac{T_1(L_\perp)}{\Delta S\, L_\perp^{d-1}\xi_2(T_1)} \tag{18}$$

As previously indicated, $\xi_2^{-1}(T_1(L_\perp))$ vanishes exponentially fast with $L_\perp$. Thus the finite-size-affected range over which the rounding occurs decreases rapidly as a function of $L_\perp$.

Having established these relations, we wish to demonstrate that they are applicable to a real symmetry-breaking transition. For the field-driven case, this has been done in considerable detail.[7,17] To the best of our knowledge, these results have not been significantly tested for the symmetry-breaking case except for the 2D q-state Potts model with $q \geqslant 5$.[10,11,19] Finite-size scaling for the Potts model is considerably more complicated than the model presented below, due to the $q+1$ degeneracy of the TM eigenvalues at the transition. Our analysis will be greatly simplified due to the symmetry of the Hamiltonian we are studying. We note that Eqs. (2) and (18) provide for a means of determining if a system is in a finite-size scaling regime. We verify that $\xi_2(T_1, L_\perp)$ has the form given in Eq. (2) and thereby calculate σ_∞. Furthermore, we demonstrate that appropriate thermodynamic quantities for systems with different $L_\perp$ collapse to a single curve when expressed as a function of the scaling variable defined in Eq. (17b), as should be expected from the scaling ansatz.

3. DEFINITION OF MODEL AND TRANSFER MATRIX FORMALISM

In order to examine the finite-size scaling ansatz presented in Section 2, we study a model originally proposed for the study of structural phase transitions.[12] The model is characterized by the Hamiltonian

$$\mathcal{H} = \sum_i V_{os}(u_i) + \sum_{\langle ij \rangle} V_c(u_i, u_j) \tag{19}$$

where

$$V_c(u_i, u_j) = \frac{k}{2}(u_i - u_j)^2 + \frac{\alpha}{4}(u_i^2 + u_j^2)(u_i - u_j)^2 \tag{20}$$

and $V_{os}(u_i)$ is the on-site potential. The scalar variable u_i is the displacement of a particle at the lattice site i. The notation $\langle ij \rangle$ indicates a sum over near-neighbor pairs; we consider only periodic boundary conditions. The on-site potential has been chosen to be the simplest on-site potential that will show a symmetry-breaking first-order transition,[12] the so-called ϕ^6 potential as a function of only one scalar variable:

$$V_{os}(u) = \frac{A}{2}u^2 - \frac{B}{4}u^4 + \frac{C}{6}u^6 \tag{21}$$

This potential is shown schematically in Fig. 2. Note that this potential is invariant under $u \to -u$. The parameters A, B, and C are positive and independent of temperature, i.e., this is a microscopic, not effective, Hamiltonian. By choosing the on-site length scale such that the absolute minima are at $u_0 = \pm 1$, the on-site potential is specified by an energy scale

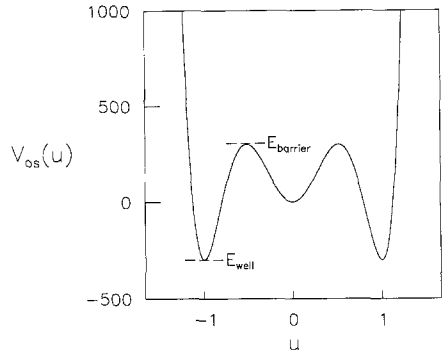

Fig. 2. The nonlinear on-site potential energy $V_{os}(u)$.

and by the ratio of the energy of the barrier (relative to the energy of the metastable minimum) to the energy at $u = u_0$. We have specified the energy scale by setting the barrier energy to $E_{\text{barrier}} = 300$. Choosing $E_{\text{barrier}}/E_{\text{well}} = 1$ defines the shape of the potential. At low temperatures the system will be localized in the side wells; at high temperatures the system is localized in the center well. The relevant order parameter is the average particle displacement $\langle u \rangle$. Two limits of this model are examined: the 5-state discrete version, in which u can take on the values ± 1, $\pm 1/2$, and 0, as well as the continuum case $-\infty < u < \infty$, relevant to structural transformations.

For the special case $\alpha = 0$ in the continuum limit, this model has only harmonic coupling between sites. Including the anharmonic coupling changes the effective harmonic coupling between the low- and high-temperature phases. This change in dispersion is an important feature of many structural phase transitions,[12] which typically undergo a large change in the phonon entropy at the transition.[20] To understand how this new term changes the effective coupling, consider a linearized theory: in the high-temperature phase, the mean-square displacement $\langle u^2 \rangle$ is small, and the anharmonic piece of the intersite coupling may be neglected. The intersite coupling then reduces to a harmonic form with force constant k. At low temperatures, when $\langle u^2 \rangle \approx 1$, the effective harmonic coupling between sites is $\sim k + \alpha$. Thus, the effective coupling force between particles in the low-temperature phase is higher than that of the high-temperature phase. (The appropriate magnitude of this intersite coupling constant, based on experiment, is discussed elsewhere.[13]) Although this argument is simplistic, a *self-consistent* harmonic calculation reproduces the exact thermodynamic quantities, found from the transfer matrix (TM) formalism, to a remarkable degree,[13] and confirms the above scenario. Higher-order corrections to this pseudoharmonic theory are the predominant source of error,[16] and in the displacive limit are less than a few percent. In the fully two-dimensional limit, the system in equilibrium will be *completely* representable by a quasiharmonic phonon theory, despite the essentially nonlinear features of the model associated with the transition. Experimental results demonstrate that this is in agreement with real systems.[20]

In the finite-size system, nonlinear excitations connecting the different phases will be macroscopically occupied in a temperature regime near the transition.[13] To understand this regime in real systems and how it changes as the system size increases, it is necessary to study a relevant model in the scaling regime. The above model with the new coupling provides an excellent model for studying the finite-size effects: *the inclusion of the new term with sufficiently large (but physically reasonable) α causes the system to be in the scaling regime even for $L_\perp = 1$.* This remarkable result will be

demonstrated more fully in Section 4. We examine the harmonic $\alpha = 0$ case and also the anharmonic case with nonzero α.

In order to study the equilibrium properties of the system, we use the TM formalism which has been developed to evaluate configurational partition functions for systems that are infinite in one direction and finite in $d-1$ directions. We present here a short introduction to the formalism; for a more complete review, along with applications to finite-size scaling, see the review by Nightingale.[21] We consider a two-dimensional system of size $L_{||} \times L_{\perp}$, with $L_{||} \to \infty$. The state of each particle may be either discrete (TM) or a continuous variable (transfer integral). We indicate the state of a particle at row i and column j by u_{ij}. As the TM and transfer integral (TI) formalisms are virtually identical, only the TM formalism will be presented.

The configurational partition function is defined to be

$$Z = \sum_{\{u_{ij}\}} \exp -\beta \mathscr{H}(\{u_{ij}\}) \tag{22}$$

where the sum is over all possible configurations of $\{u_{ij}\}$. In order to simplify this equation, we first label the state of a *row* of particles by x_j, thus specifying the configuration of all $L_{\perp}$ particles. Note that if each particle has m distinct states, the number of allowed configurations for x_j is $m^{L_{\perp}}$. The Hamiltonian may then be written in the form

$$\mathscr{H} = \sum_{i=1}^{L_{||}} V_1(x_i) + V_2(x_i, x_{i+1}) \tag{23}$$

The TM is defined to be

$$\tilde{T}(x_i, x_j) = \exp\{-\beta[\tfrac{1}{2}V_1(x_i) + \tfrac{1}{2}V_1(x_j) + V_2(x_i, x_j)]\} \tag{24}$$

As the TM is real and symmetric, it has real eigenvalues λ_n. We are free to label our eigenvalues such that

$$\lambda_0 > \lambda_1 \geqslant \lambda_2 \geqslant \cdots \geqslant 0 \tag{25}$$

Enforcing periodic boundary conditions along the "parallel" direction enables us to write the configurational partition function as

$$Z = \sum_n \lambda_n^{L_{||}} \tag{26}$$

Assuming that λ_0 is not degenerate with the other eigenvalues, the partition function is, in the thermodynamic limit,

$$Z_{L_{||} \to \infty} = \lambda_0^{L_{||}} = e^{-\beta G(L_{\perp}, L_{||})} \tag{27}$$

This gives a reduced Gibbs free energy per particle of

$$g = \frac{G}{L_{||} L_{\perp} T} = -\frac{1}{L_{\perp}} \ln \lambda_0 \tag{28}$$

Thermodynamic quantities, such as the specific heat, entropy, and internal energy, may be determined from the temperature derivatives of g.

We also define the TM correlation lengths ξ_j, $j = 1, 2, \ldots$, by the relation

$$\xi_j^{-1} \equiv -\ln(\lambda_j/\lambda_0) \tag{29}$$

Note that if we define the reduced energies [in analogy to Eq. (28)]

$$g_j \equiv -\frac{1}{L_{\perp}} \ln \lambda_j \tag{30}$$

then the inverse correlation lengths correspond to the differences between the reduced energies per strip.

When two or more phases may coexist, the dominant eigenvalue becomes degenerate, the degeneracy being equal to the number of possible phases.[17] The first-order phase transition is associated with a crossing of eigenvalues.[7,14,17] Equivalently, one or more of the correlation lengths ξ_j become infinite [Eq. (29)]. For symmetry-breaking transitions, the fact that ξ_1 becomes infinite for $T \leqslant T_1$ in the bulk limit is consistent with the fact that the symmetry-broken states have identical free energies. This will not occur for systems of finite size; however, in the scaling regime, there will be *near* degeneracies, with associated eigenvectors related to probabilities in the various phases. The correlation lengths that diverge as $L_{\perp} \to \infty$ are the length scales corresponding to the domain wall separation. These correlation lengths are the appropriate lengths that were introduced in Section 2.

In Fig. 3c the reduced energies $g_j = -(1/L_{\perp}) \ln \lambda_j$, $j = 0, 1, 2$, are shown for our continuum model with $\alpha = k = 40{,}000$ and $L_{\perp} = 1$ as a function of temperature (to be discussed more fully in Section 4). Here, the near degeneracy is apparent: note that the function g_0 corresponding to the true free energy shows a rounded cusp in the "mixing" (viz., the finite-size-affected) region. The indicated inverse correlation lengths ξ_1^{-1} and ξ_2^{-1} both vanish as $L_{\perp} \to \infty$. We note that ξ_2 is the correlation length associated with domain walls between center and side wells, as discussed in Section 2. These walls will have lower associated free energy than domain walls between the symmetry-broken states. This, along with Eq. (2), indicates that $\xi_2 < \xi_1$.

For finite $L_\perp$ the dominant eigenvalue will be nondegenerate at all $T>0$ (i.e., there will be no phase transition), except in the $L_\perp \to \infty$ limit, where the system is fully two dimensional.[22] (For Hamiltonians with continuous symmetries, there is no transition except in fully three-dimensional systems.[23]) To understand the avoided crossings in the finite-size system, it is useful to consider a simplified form of the TM similar to those discussed in refs. 14 and 17. At $T=T_1(L_\perp)$ the TM is (in the appropriate basis)

$$\tilde{T}=\lambda_0 \operatorname{diag}(1, e^{-\xi_1^{-1}}, e^{-\xi_2^{-1}},\ldots) \tag{31}$$

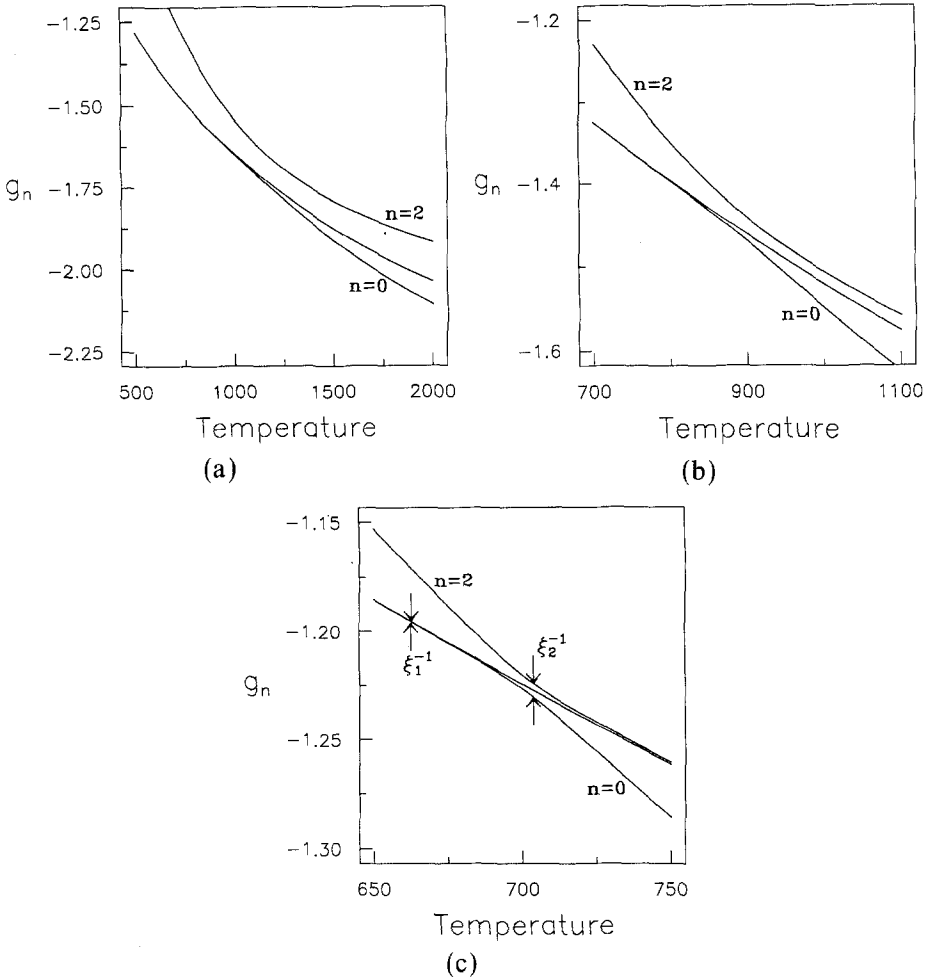

Fig. 3. Reduced free energies g_0, g_1, and g_2 for the $L_\perp=1$ continuum model. The anharmonic coupling strengths are (a) $\alpha/k=0$, (b) $\alpha/k=0.5$, and (c) $\alpha/k=1$.

For sufficiently large $L_\perp$ we know that for our system $\xi_2 \gg \xi_3$ because ξ_3 remains finite as $L_\perp$ diverges; this suggests a *phenomenological* reduction of the matrix to a 3×3 form, where the $L_\perp \to \infty$ limits of the eigenvalues are mixed (due to the formation of domain walls) in the finite-size system. As we will show, this reduction utilizes the symmetries of the Hamiltonian and incorporates the loss of long-range order in finite systems due to domain wall formation. From this reduced TM we form an explicit expression for the free energy that approaches the correct limit away from the finite-size-affected regime, and has a singular part that obeys the scaling ansatz presented in Section 2.

In Fig. 1 we have denoted the reduced energy densities for domain walls between regions with $\langle u \rangle > 0$ and $\langle u \rangle = 0$ as σ_{+0}, between different low-temperature phase variants as σ_{+-}, etc. Imposing the symmetries of the Hamiltonian, specifically $\mathcal{H}(\{u_{ij}\}) \to \mathcal{H}(\{-u_{ij}\})$, generates relations between the domain-wall free energies:

$$\sigma_{+0} = \sigma_{-0} = \sigma_{0-} = \sigma_{0+}, \qquad \sigma_{+-} = \sigma_{-+} \tag{32}$$

We thus suggest the *approximate* form of the TM[17]

$$\tilde{T} = e^{-L_\perp g_L} \begin{pmatrix} 1 & \Delta_2 & \Delta_1 \\ \Delta_2 & e^{-L_\perp \Delta g} & \Delta_2 \\ \Delta_1 & \Delta_2 & 1 \end{pmatrix}, \qquad \Delta g \equiv g_H(T) - g_L(T) \tag{33}$$

where the basis vectors $(1\ 0\ 0)^T$ and $(0\ 0\ 1)^T$ represent the low-temperature phase variants, and $(0\ 1\ 0)^T$ represents the high-temperature phase. One may picture each of these corresponding to Gaussian order-parameter distributions $P(u)$ centered in the appropriate local minimum of the on-site potential. The function $g_L(T)$ corresponds to the Gibbs free energy of the *bulk* system for $T < T_1$, and the function $g_H(T)$ is the free energy for the bulk system for $T > T_1$. Note that both functions are analytic throughout their complementary temperature domains, and thus are defined over the entire temperature range. The "mixing parameters" are

$$\begin{aligned} \Delta_1 &= \frac{1}{2} \xi_1^{-1} \sim \exp(-\sigma_{+-} L_\perp) \\ \Delta_2 &= \frac{1}{2\sqrt{2}} \xi_2^{-1} \sim \exp(-\sigma_{+0} L_\perp) \end{aligned} \tag{34}$$

Furthermore, we expect on physical grounds that $\sigma_{+-} > \sigma_{+0}$. This implies that $\Delta_1 \ll \Delta_2$.

To elucidate the motivation for this form, we first block-diagonalize this matrix using the unitary transformation

$$U=\frac{1}{\sqrt{2}}\begin{pmatrix}1 & 0 & 1\\ 0 & \sqrt{2} & 0\\ 1 & 0 & -1\end{pmatrix} \tag{35}$$

This transformation expresses the TM in a basis which includes symmetric and antisymmetric combinations of vectors representing the two variants of the low-temperature phase as well as the (necessarily symmetric) high-temperature phase. The irreducible form of the TM is then

$$\tilde{T}=e^{-L_\perp g_L}\begin{pmatrix}1+\Delta_1 & \sqrt{2}\,\Delta_2 & 0\\ \sqrt{2}\,\Delta_2 & e^{-L_\perp \Delta g} & 0\\ 0 & 0 & 1-\Delta_1\end{pmatrix} \tag{36}$$

Noting that we expect Δ_1 to be very small, this form shows that the dominant mixing in the region of the transition ($\Delta g \approx 0$) is due to Δ_2. The 2×2 block is identical in form to the form argued for the field-driven case,[7,17] if we neglect Δ_1. This indicates that the dominant finite-size effects near T_1 are due to the formation of domain walls between the high- and low-temperature states. Thus, although there is three-phase coexistence in the bulk limit, the predominant finite-size effects near T_1 can be understood by consideration of only two eigenvalues of the TM, viz. the largest eigenvalues associated with eigenvectors that are invariant under the symmetries of the Hamiltonian. In general, a similar reduction will occur for systems breaking a p-fold degeneracy, with the dominant mixing due to the shortest of the diverging length scales, namely ξ_p.

Diagonalizing the above matrix in terms of the variable

$$x=[(1+\Delta_1-e^{-L_\perp \Delta g})^2+8\Delta_2^2]^{1/2} \tag{37}$$

we find the eigenvalues

$$\begin{aligned}\lambda_0&=\tfrac{1}{2}e^{-L_\perp g_L}(1+\Delta_1+e^{-L_\perp \Delta g}+x)\\ \lambda_1&=e^{-L_\perp g_L}(1-\Delta_1)\\ \lambda_2&=\tfrac{1}{2}e^{-L_\perp g_L}(1+\Delta_1+e^{-L_\perp \Delta g}-x)\end{aligned} \tag{38}$$

We examine these results for three limiting cases.

In the limit that $e^{-L_\perp \Delta g}$ is small, i.e., $g_L < g_H$, we find

$$x=1+\Delta_1-e^{-L_\perp \Delta g}+\mathcal{O}(\Delta_2^2, e^{-2L_\perp \Delta g}) \tag{39}$$

The reduced energies $g_j \equiv -L_\perp^{-1} \ln \lambda_j$ are then

$$\begin{aligned} g_0 &= g_L - \Delta_1 + \mathcal{O}(\Delta_2^2, e^{-2L_\perp \Delta g}) \\ g_1 &= g_L + \Delta_1 + \mathcal{O}(\Delta_1^2) \\ g_2 &= g_H + \mathcal{O}(\Delta_2^2, e^{-2L_\perp \Delta g}) \end{aligned} \tag{40}$$

Thus, at low temperatures, the actual free energy g_0 is very close to that of the bulk system.

The second case, appropriate when $T > T_1$ and therefore $g_H > g_L$, is when $e^{-L_\perp \Delta g} \gg 1$. In this case, the reduced free energies are

$$\begin{aligned} g_0 &= g_H + \mathcal{O}(\Delta_2^2, e^{2L_\perp \Delta g}) \\ g_1 &= g_L + \Delta_1 + \mathcal{O}(\Delta_1^2) \\ g_2 &= g_L - \Delta_1 + \mathcal{O}(\Delta_2^2, e^{2L_\perp \Delta g}) \end{aligned} \tag{41}$$

These are identical to the values in the low-temperature case [Eq. (40)], except that the true free energy g_0 now corresponds to the high-temperature phase.

Lastly, near the transition where the functions g_L and g_H cross, the value of $e^{-L_\perp \Delta g}$ will be nearly equal to 1. Denoting the entropies of the low- and high-temperature phases by S_L and S_H, respectively, we have

$$g_L = g_b(T_1) - tS_L + \mathcal{O}(t^2), \qquad g_H = g_b(T_1) - tS_H + \mathcal{O}(t^2) \tag{42}$$

where $g_b(T_1)$ is the bulk free energy at the transition. The eigenvalues, to lowest order in t, are

$$\begin{aligned} g_0 &= g_b(T_1) - \frac{t}{2}(S_L + S_H) - \frac{1}{2}\Delta_1 - \frac{1}{2L_\perp \xi_2}\left(\frac{1}{4} y_t^2 + 1\right)^{1/2} \\ &\quad + \mathcal{O}(\Delta_1^2, \Delta_2^2) \\ g_1 &= g_b(T_1) - tS_L + \Delta_1 + \mathcal{O}(\Delta_1^2) \\ g_2 &= g_b(T_1) - \frac{t}{2}(S_L + S_H) - \frac{1}{2}\Delta_1 + \frac{1}{2L_\perp \xi_2}\left(\frac{1}{4} y_t^2 + 1\right)^{1/2} \\ &\quad + \mathcal{O}(\Delta_1^2, \Delta_2^2) \end{aligned} \tag{43}$$

Here, we have used the scaling variable $y_t = t\,\Delta S\, L_\perp \xi_2$ as defined in Eq. (17b). Note that g_0 and g_2 are both singular in the $L_\perp \to \infty$ limit, though both also contain identical analytic contributions. The nonanalytic contributions are given by

$$g_s \equiv g_0 - g_2 = -\frac{1}{L_\perp \xi_2}\left(\frac{1}{4} y_t^2 + 1\right)^{1/2} \tag{44}$$

which has the scaling form given in Eq. (17b). This demonstrates how the analytic function g_0 is rounded over a range specified by ξ_2, which is determined from the reduced domain wall energy. As $L_\perp$ diverges, this function approaches the singular bulk free energy $g_b(T)$ specified by

$$g_b(T) = \min(g_L, g_H) \tag{45}$$

4. NUMERICAL TESTS OF FINITE-SIZE SCALING

4.1. Continuum Case, $L_\perp = 1$

We present the 1D continuum limit in order to demonstrate that the model has near degeneracies in its TM spectrum, as discussed in the preceding section. Furthermore, this serves to make the above concepts more concrete. The narrow rounding regime of the transition in the $L_\perp = 1$ limit shows why this model is ideal for studying finite-size effects in first-order symmetry-breaking transitions. This remarkable behavior of the model in one dimension has been previously noted.[13]

The spectrum has been calculated by discretizing the one-particle states and then calculating the dominant eigenvalues of the associated TM via the conjugate gradient method.[21] We tested the convergence of the transition temperature and ξ_2^{-1} versus the number of discrete states, and found that a minimum of 25 states were required before the results were essentially independent of the number of states. We have chosen the parameters of the model so that the scaling as a function of $L_\perp$ may be easily demonstrated: *it is important to realize that these parameters may be chosen so that the 1D results are arbitrarily close to a true transition.*[13] Specifically, increasing the coupling constants k and α has the effect of narrowing the finite-size-affected regime to an arbitrarily small amount by decreasing the value of ξ_2^{-1}. Our particular choice of parameters allows for eigenvalues that are very nearly degenerate, while still maintaining numerical accuracy. Note that for $L_\perp = 1$, the inclusion of the anharmonic coupling term is necessary (cf. Fig. 3) for the system to show the behavior close to that of a true transition. This will be rigorously proved in the analytic treatment of the 1D system presented in Section 5.

Figure 3 shows the free energies $g_j \equiv -\ln \lambda_j$ corresponding to the three dominant values of the TM spectrum, for $L_\perp = 1$ and $\alpha = 0$, $k/2$, k. The effect of α is to reduce $T_1(L_\perp)$ as well as to reduce the gap ξ_2^{-1}. Corresponding to this reduced gap, the finite-size-affected regime is smaller, as indicated in Eq. (18). There are two reasons the reduction of ξ_2^{-1} is to be expected. First, the increased coupling suggests that the domain walls will

have a higher energy. More importantly, increasing the value of α lowers the entropy of the low-temperature phase. This stabilizes the high-temperature phase, as demonstrated by the lower transition temperature. The decreased transition temperature increases the *reduced* domain wall energy significantly. As ξ_2 grows exponentially with this reduced energy, the finite-size-affected regime becomes very narrow—this is the reason that α makes the model reach the scaling regime for small $L_\perp$.

One of the most important quantities that we are concerned with is the probability for finding a strip in the state x_i; this is given by

$$P(x_i) = |\phi_0(x_i)|^2 \tag{46}$$

where $\phi_0(x_i)$ is the eigenvector corresponding to the dominant eigenvalue. As x_i specifies the states of $L_\perp$ particles in the strip i, $P(x_i)$ is a joint probability. To find the probability of finding a particular particle in a given state u_{ij}, it is necessary to integrate out the possible configurations of the other particles within the strip. Specifically, we have

$$P(u_{ij}) = \sum_{\{u_{ik}, k \neq j\}} P(x_i = \{u_{i1} \cdots u_{iL_\perp}\}) \tag{47}$$

For the $L_\perp = 1$ system the eigenfunction $\phi_0(u)$ corresponding to g_0 is the probability amplitude of finding a particular particle with a displacement u, i.e., $P(u) = |\phi_0(u)|^2$. This eigenfunction, shown in Fig. 4a, indicates that at low temperatures the system is localized in the side wells of the potential; at higher temperatures, the system will be predominantly located in the center well. The eigenfunction $\phi_1(u)$ is shown in Fig. 4b. At low temperatures the eigenvalue λ_1 is very nearly degenerate with λ_0, becoming fully degenerate at $T = 0$ in one dimension and at $T = T_1$ in two dimensions. The structure of these eigenfunctions is entirely consistent with the idea of the mixing of two symmetry-broken probability amplitudes due to the finite size of the system. In Fig. 4c, the third eigenfunction $\phi_2(u)$ is shown. For $T \approx T_1 (L_\perp = 1)$ we see the evidence of the mixing of the *symmetric* eigenfunctions $\phi_0(u)$ and $\phi_2(u)$, in strong agreement with the phenomenological form in Eq. (33). This mixing occurs only in the finite-size-affected regime near T_1. The multiple peaks at $u = \pm 1$ and at $u = 0$ indicate that this is the coexistence regime. Again, this supports the phenomenological form of the TM given in Eq. (33). One clearly sees the band repulsion produced by the symmetric–symmetric coupling. For temperatures near T_1, but outside of the finite-size-affected regime, the overlap of the probability densities $\phi_0^2(u)$ and $\phi_2^2(u)$ will be small. In the bulk limit, there will be *no* overlap except at T_1, indicating the lack of joint occupation between the two phases away from the transition.[2]

4.2. Five-State Case

In order to demonstrate the scaling form in the crossover to two dimensions we initially examine the five-state case. This is the limit in which there are only five discrete states that the local order parameter may assume: $u_{ij} = \pm 1, \pm 0.5, 0$. Due to the limited number of states in this case, the numerics is more convenient than for the continuum case. We are effectively limited to $L_\perp \leqslant 6$ due to the size of the TM. We first establish that there is a first-order transition for the 5-state case, and also that the scaling ansatz given in Eq. (17b) is valid even for small $L_\perp$. To do this, we show the entropy as a function of temperature for each value of $L_\perp$ in Fig. 5 as a function of the scaling variable y_t given in Eq. (17b). Clearly, as $L_\perp$ increases, the data collapse onto a single curve, with the entropy changing rapidly over the range ΔT [cf. Eq. (18)]. As discussed in Section 2, this

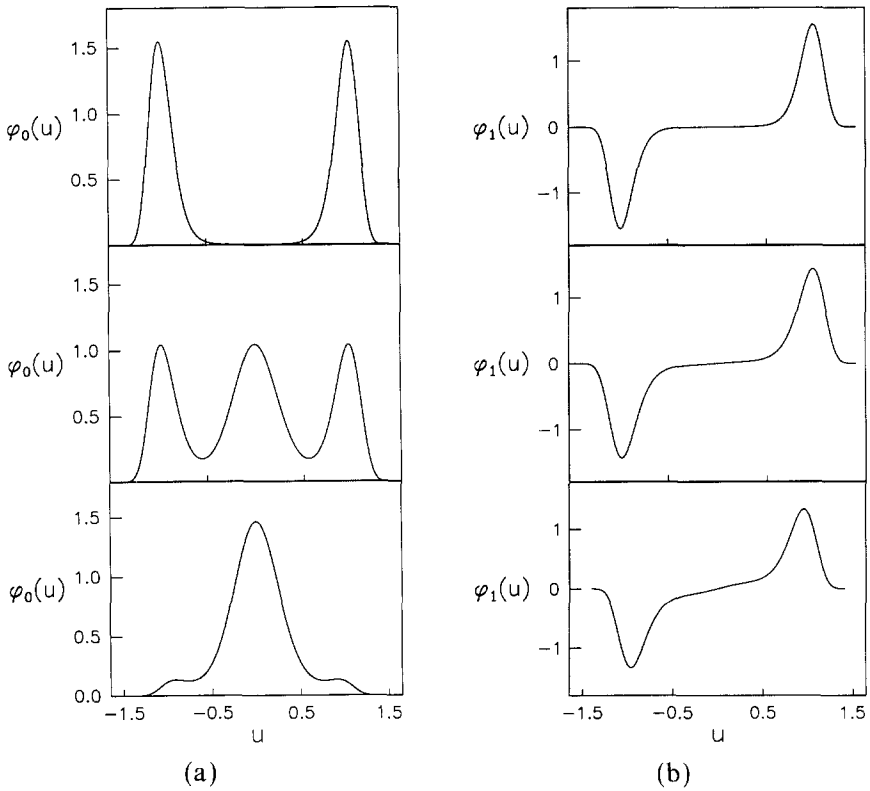

Fig. 4. (a) Transfer matrix eigenfunction $\phi_0(u)$ for the $L_\perp = 1$ case, at $T < T_1$ (top graph), $T \approx T_1$ (center graph), and $T > T_1$ (bottom graph). (b) Same as (a), but $\phi_1(u)$. (c) Same as (a), but $\phi_2(u)$.

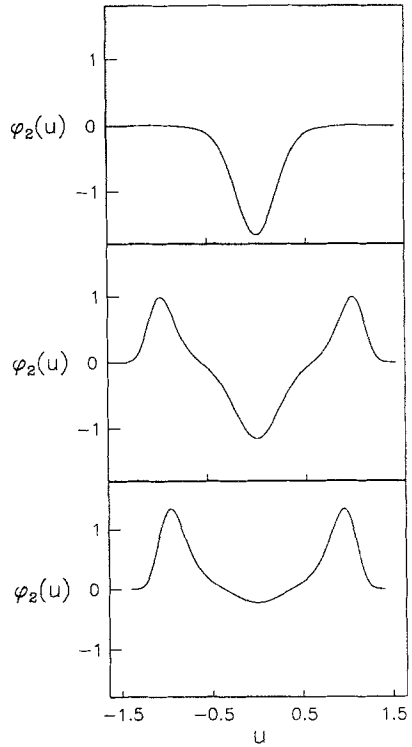

Fig. 4. (*Continued*)

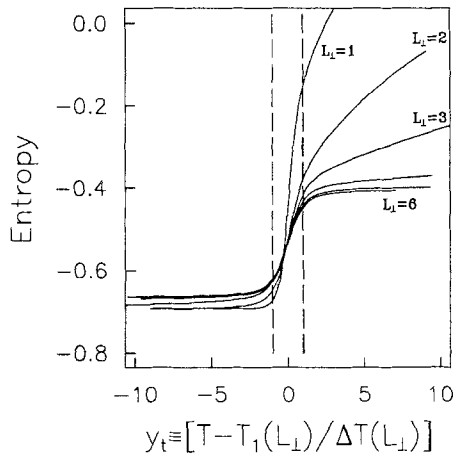

Fig. 5. Entropy versus scaling variable $y_t = t\,\Delta S\,L_\perp \xi_2$ for $1 \leqslant L_\perp \leqslant 6$ for the five-state model.

temperature range vanishes exponentially fast as a function of $L_\perp$. Thus, in the $L_\perp \to \infty$ limit, there will be a discontinuity in the entropy at $T = T_1(L_\perp)$. This verifies that a first-order transition occurs in the bulk limit. In Table I we also show T_1, ξ_2^{-1}, and ΔT [as defined in Eq. (18)] as a function of $L_\perp$. For $\alpha = k$, the reduction of ΔT is quite dramatic.

To test the scaling form of the correlation length ξ_2, we write Eq. (2) in the form

$$\ln \xi_2(T_1(L_\perp), L_\perp) = C + w \ln(L_\perp) + \sigma_\infty L_\perp \tag{48}$$

Figure 6 shows the fit to this form, for the harmonic coupling case $\alpha = 0$ and for the anharmonic cases $\alpha = k/2$ and $\alpha = k$. Clearly, the fit is good in all cases. The limiting slope in the large-$L_\perp$ limit is larger for $\alpha = k$ than for $\alpha = 0$ by a factor of ~ 5. This increase in σ_∞ causes a dramatically increased value for ξ_2; this strongly decreases the temperature range over which the finite-size effects are significant, viz. the finite-size-affected region. Thus, we see that the anharmonic coupling brings the system into this regime by increasing the interfacial free energy of domain walls between the high- and low-temperature phases.

One feature of Fig. 6 that is perplexing is the positive curvature, which implies from Eq. (48) that the exponent w is negative; this seems counterintuitive. Again, note that for the field-driven transition in the Ising model,

Table I. Transition Temperature, Inverse Domain-Wall Correlation Length, and Width of Finite-Size-Affected Regime Versus $L_\perp$ for Five-State System

$L_\perp$	T_1	ξ_2^{-1}	ΔT
$k = \alpha = 40{,}000$; $\Delta S = 0.256$			
1	2588.0	0.0478003	483.0
2	4785.0	0.03415	319.0
3	5627.0	0.01133381	83.0
4	5848.0	0.002585	14.8
5	5905.8	0.0005132	2.37
6	5921.10	0.0000996	0.384
$k = 40{,}000$; $\alpha = 0$; $\Delta S = 0.3$			
1	2180.0	0.118817	870.0
2	4170.0	0.113577	790.0
3	5300.0	0.09291	550.0
4	5809.0	0.0713878	350.0
5	6070.0	0.05369	210.0
6	6210.0	0.0396	130.0

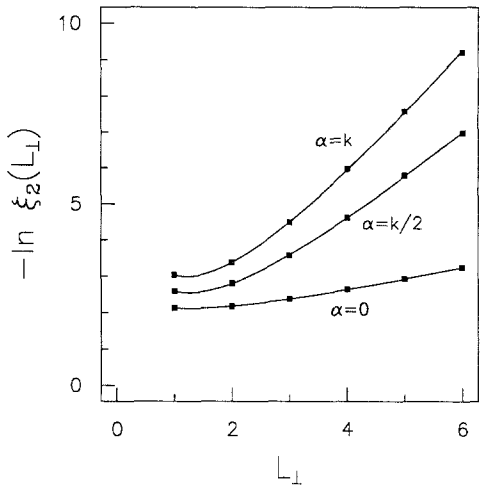

Fig. 6. Fit of $\ln \xi_{||}$ for $\alpha = 0$, $\alpha = k/2$, and $\alpha = k$ for the five-state model. The limiting slopes, correspond to the reduced interfacial energies, are $\sigma(\alpha = 0) = 0.403$, $\sigma(\alpha = k/2) = 1.60$, and $\sigma(\alpha = k) = 2.21$.

the exponent has the value $w = 1/2$. Part of this may be explained by noting that each data point is at a different temperature, and this may significantly affect the surface free energy. Also note that the scaling of $\sigma(L_\perp)$ is different than the actual scaling of the domain-wall free energy per length, as this is the domain-wall free energy divided by the cross-sectional length $L_\perp$.[7] In general, the interpretation of $\sigma(L_\perp)$ is difficult: in the exactly solvable model,[3] the analogous quantity is neither a domain-wall free energy nor an inverse bulk correlation length. Although we believe that for our model this quantity is associated with the domain-wall free energy, further study is necessary to understand its approach to the bulk limit.

4.3. Continuum Limit, $L_\perp \geqslant 1$

Now that we have demonstrated the effectiveness of the scaling ansatz [Eq. (17b)] in describing the effects of finite $L_\perp$, we return to the continuum limit. In this limit the vibrational entropy effects of the new term discussed in Section 3 are relevant. We are limited to $L_\perp = 1, 2, 3$, again due to the size of the TM. In Table II, we show T_1, ξ_2, and ΔT as a function of $L_\perp$ for the continuum model. Note that $\Delta T(L_\perp = 3)$ is *five orders of magnitude less* than $\Delta T(L_\perp = 1)$ for the $\alpha = k$ case; for $\alpha = 0$, the reduction is a mere factor of two. Comparison of this with Table I shows several noteworthy points. First, for a given $L_\perp$, the rounding regime is much smaller for the continuum model. Also, the transition temperature is

Table II. Transition Temperature, Inverse Domain-Wall Correlation Length, and Width of Finite-Size-Affected Regime Versus $L_\perp$ for Continuum System

$L_\perp$	T_1	ξ_2^{-1}	ΔT
$k = \alpha = 40{,}000$; $\Delta S = 0.37$			
1	702.375	0.0061659076	11.6
2	763.90	0.00008231	0.0855
3	795.05610	0.000000882	0.000632
$k = 40{,}000$; $\alpha = 0$; $\Delta S = 0.05$			
1	1172.0	0.09071	2126.0
2	2128.0	0.07769	1653.0
3	2850.0	0.0711	1350.0

considerably lower. We attribute the lower transition temperature to the relatively high vibrational entropy in the high-temperature phase; this does not play a role in the five-state case. Due to the significantly lower transition temperature, the reduced surface free energy σ_∞ is considerably larger for the continuum case than for the five-state model. Fitting ξ_2 to the form in Eq. (48) gives a value for σ_∞ that is roughly five times that of the five-state model. This increased value explains the smaller value of ξ_2^{-1} and therefore the narrow rounding regime [cf. Eq. (18)].

To demonstrate that the finite-size scaling ansatz is satisfied extremely well for this model, Fig. 7 shows $\langle u^2 \rangle$ versus the scaling variable y_t introduced in Eq. (17b). In the $L_\perp \to \infty$ limit, this will have a discontinuity at the transition. The curves for $L_\perp = 1, 2, 3$ are quite close, proving the

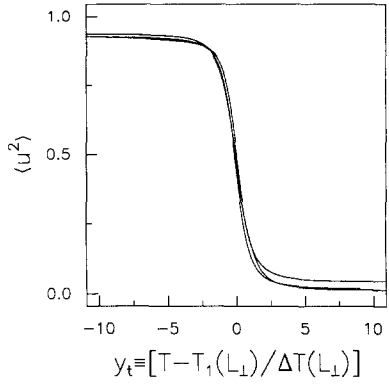

Fig. 7. Average square order parameter $\langle u^2 \rangle$ versus scaling variable y_t for the continuum model, for $L_\perp = 1, 2, 3$.

validity of the ansatz in describing our system. Note that $\langle u^2 \rangle$ rapidly approaches the $T=0$ value $\langle u^2 \rangle = 1$, indicating that the transition will be strongly first-order.

It is instructive to note that the latent heat of the continuum model is very close to the energy difference between the absolute minimum and the metastable minimum of the on-site potential. This result is independent of α, and is due to the fact that the system behaves like a harmonic solid away from the transition:[13,16] in either the low- or high-temperature phase, the average potential energy per particle is approximately $\frac{1}{2}T$ above the appropriate minimum in $V_{os}(u)$, so that the difference in internal energies between the phases is quite close to the $T=0$ difference, E_{well}.

In ref. 12 it was noted that $P(u)$ showed heterophase fluctuations near the temperature T_1. In $L_\perp = 2$ and 3 the convergence to the bulk limit, where the fluctuations vanish, is becoming clear. Figure 8 shows $P(u)$ at $T = T_1(L_\perp) \pm 3$ for $L_\perp = 1$ and 2. Note that while the indications of heterophase fluctuations are clear for $L_\perp = 1$, there are *no* such indications for $L_\perp = 2$—such fluctuations only occur over a temperature range given

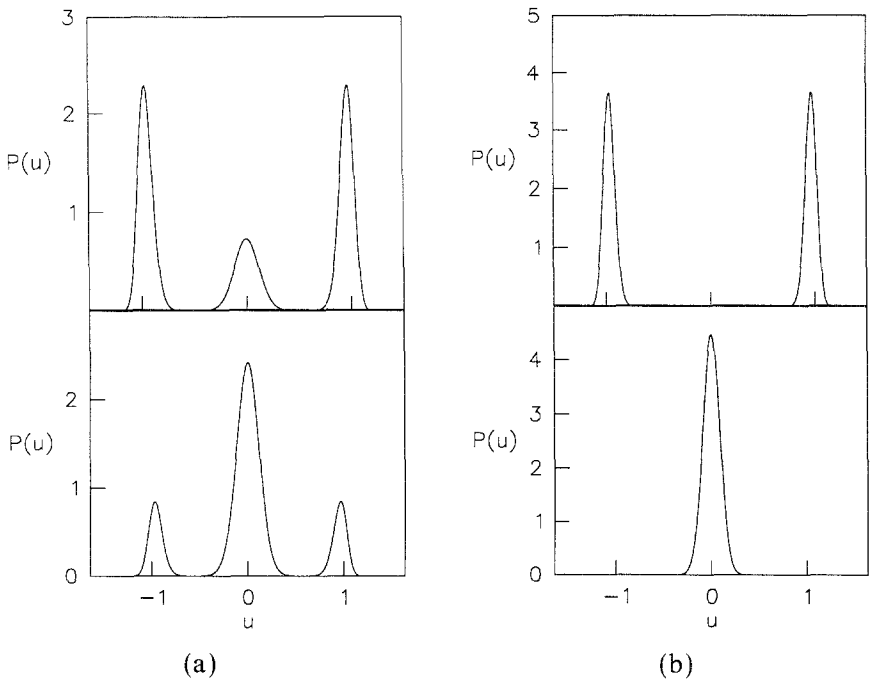

Fig. 8. (a) Probability distribution $P(u)$ for $L_\perp = 1$ at $T = T_1 - 3$ (top graph) and $T = T_1 + 3$ (bottom graph). (b) Probability distribution $P(u)$ for $L_\perp = 2$ at $T = T_1 - 3$ (top graph) and $T = T_1 + 3$ (bottom graph).

approximately by $\Delta T(L_\perp)$ around the temperature $T_1(L_\perp)$. As suggested elsewhere,[2] and rigorously shown here (see Section 3), there are no heterophase fluctuations away from the transition temperature for systems in thermodynamic equilibrium.

5. THE PSEUDO-SCHRÖDINGER APPROACH

For the continuum model, an analytic approach to the TI has been developed[24–26] for the so-called strong-coupling limit. This work has primarily concentrated on the sine-Gordon chain and the one-dimensional ϕ^4 system. For these cases, a phenomenology has been developed for the statistical mechanics incorporating both phonon excitations as well as nonlinear topological excitations, viz. a dilute soliton gas. By proper incorporation of the total degrees of the system, and including the effect of kinks on the phonon density of states, the phenomenological free energy associated with the kinks is identical to the splitting between the dominant eigenvalues.[26,27] This demonstrates that the gap between dominant eigenvalues is indeed due to domain walls, as argued previously.

By following a similar approach, we shall demonstrate that for the continuum model in one dimension, the TI eigenvalue problem can be reduced to a one-dimensional Schrödinger equation in the strong-coupling or "displacive"[15] limit. We write the on-site potential in the form

$$V_{\text{os}}(u) = V_0 \tilde{V}(u), \qquad \tilde{V}(u) \equiv (u^2 - 1)^2 (u^2 + E_g) \tag{49}$$

to introduce the characteristic energy scale V_0. Note that the value $V_0 E_g$ is equal to the well depth E_{well} indicated in Fig. 2. The displacive limit corresponds to

$$d \equiv \left(\frac{k}{V_0} \right)^{1/2} \gg 1 \tag{50}$$

The parameter d is a length scale (relative to the lattice spacing) that determines the importance of the lattice discreteness. In the limit $d \gg 1$ the displacement u only changes by small amounts between lattice sites and therefore may be considered a continuous function of position along the lattice.

In terms of the symmetric kernel

$$K(u_i, u_{i+1}) \equiv \frac{1}{2} V_0 [\tilde{V}(u_i) + \tilde{V}(u_{i+1})] + \frac{1}{2} k (u_i - u_{i+1})^2$$

$$+ \frac{\alpha}{4} (u_i^2 + u_{i+1}^2)(u_i - u_{i+1})^2$$

the TI eigenvalue problem is

$$\int du_i\, K(u_i, u_{i+1})\, \phi_n(u_i) = \lambda_n \phi_n(u_{i+1}) \tag{51}$$

In the Appendix, we demonstrate that for large d and small α/k this may be reduced to the form of a pseudo-Schrödinger equation

$$\left(-\frac{1}{2m^*}\frac{\partial^2}{\partial x^2} + \tilde{V}(x) + V(T) + \tilde{\alpha} T x^2 \right) \phi(x) = \varepsilon_n \phi_n(x) \tag{52}$$

representing a particle of mass m^* in an effective potential

$$V_{\text{eff}}(x) = \tilde{V}(x) + V(T) + \tfrac{1}{2}\tilde{\alpha} T x^2 \tag{53}$$

(Clearly, this is similar to a Landau form for the free energy.) The variables in Eq. (52) are defined as

$$V(T) = -\frac{T}{2V_0} \ln\left(\frac{2\pi T}{k}\right), \qquad \tilde{\alpha} = \frac{\alpha}{2kV_0}, \qquad m^* = kV_0\beta^2 \tag{54}$$

The eigenvalues ε_n of the pseudo-Schrödinger equation are related to the values of λ_n by

$$\lambda_n = \exp(-\beta V_0 \varepsilon_n) \tag{55}$$

Note that this definition is equivalent to

$$\varepsilon_n = \frac{T}{V_0} g_n \tag{56}$$

where g_n are the reduced energies from Eq. (30). The free energy of the system is given by

$$G/N = V_0 \varepsilon_0 \tag{57}$$

Thus, for the one-dimensional model, finding the free energy of the system is equivalent to finding the ground state associated with the pseudo-Schrödinger equation. (Note that a similar approach has been used to derive the exponent w for the Kac model;[28] however, a similar calculation does not appear possible for this model.)

It is useful no note some formal aspects of the pseudo-Schrödinger equation at this point. The usual models that have been studied using this technique have had only harmonic intersite couplings, i.e., $\alpha = 0$. In this case, the differences between eigenvalues are universal functions of the

combination $m^* = kV_0/T^2$; the effect of changing either k or V_0 on gaps in the spectrum is merely the result of rescaling energies. The anharmonic coupling creates a new, adjustable energy scale that directly affects the physics of the problem, viz. the energy gaps, and allows for the study of finite-size effects for small $L_\perp$.

The simplest way to understand the features of the spectrum of the pseudo-Schrödinger equation is by simple estimates for the ground-state energy. At low temperatures (large m^*) we may find approximate solutions by assuming that the system is isolated in one of the side wells. We may then approximate the potential V_{eff} by the harmonic form

$$V_{\text{eff}}(x) \approx V_{\text{eff}}(\pm 1) + \tfrac{1}{2} V''_{\text{eff}}(\pm 1)(x \mp 1)^2 \tag{58}$$

The approximate ground-state energy resulting from this is

$$\varepsilon_{\text{side}} \approx V(T) + V_{\text{eff}}(\pm 1) + \frac{1}{2}\left[\frac{V''_{\text{eff}}(\pm 1)}{m^*}\right]^{1/2} \tag{59}$$

Similarly, a separate approximate solution corresponds to the particle located in the central well. Approximating the potential by

$$V_{\text{eff}}(x) \approx V_{\text{eff}}(0) + \tfrac{1}{2} V''_{\text{eff}}(0)\, x^2 \tag{60}$$

we obtain the resulting energy

$$\varepsilon_{\text{center}} \approx V_{\text{eff}}(0) + \frac{1}{2}\left[\frac{V''_{\text{eff}}(0)}{m^*}\right]^{1/2} + V(T) \tag{61}$$

These values correspond to the free energy of the model within the harmonic approximation. The curvature of $\tilde{V}(u)$ near $u = \pm 1$ is greater than that near $u = 0$ (roughly by a factor of four); therefore these two solutions cross at a temperature T_1 given by

$$E_g + \frac{T_1}{2}\left[\frac{\tilde{V}''(0)}{kV_0}\right] = \frac{\alpha}{4kV_0} T_1 + \frac{T_1}{2}\left[\frac{\tilde{V}''(\pm 1) + \alpha T_1/2kV_0}{kV_0}\right]^{1/2} \tag{62}$$

Equation (62) provides an estimate of T_1 for the 1D system, demonstrating that the transition temperature is strongly affected by the strength of the anharmonic coupling. Note that the parameter α only affects the side-well solution; by including α, the estimated transition temperature is lowered. As the zero-point energy of the side-well states is higher than that for the center-well state, an upper bound on T_1 may be made by neglecting the "zero-point" energy. This gives the estimate $E_g \approx \alpha T_1/4kV_0$, which gives the approximate behavior $T_1 \lesssim 4E_g kV_0/\alpha$, proving that $T_1 \to 0$ as α diverges. In Fig. 9, the prediction for T_1 from Eq. (62) is shown as a function of α/k. This shows the correct qualitative behavior: the high-temperature phase

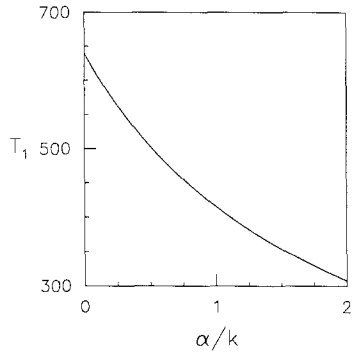

Fig. 9. Transition temperature T_1 for the 1D model as a function of α/k, predicted using Eq. (62).

may be stabilized to arbitrarily low temperatures by choosing a sufficiently large α.

In the true spectrum, there is no level crossing (as discussed in Section 3). Near T_1, the symmetric linear combination of side-well states mixes with the symmetric, nodeless central well state, forming the gap related to ξ_2^{-1} [see Eq. (43)]. The gap in the spectrum between these levels may be calculated using the WKB approximation. We assume that we may construct *approximate* solutions $\phi_{\text{side}}(x)$ (even in x and localized in the side wells) and $\phi_{\text{center}}(x)$ (localized in the central well). At $T = T_1$ these have the same (approximate) energy ε. We define x_0 and x_2 to be the classical turning points[29] specified by

$$\tilde{V}(x_0) = \tilde{V}(x_2) = \varepsilon, \qquad 0 < x_0 < x_2 < 1 \tag{63}$$

The tunnel splitting of the states produces the approximate eigenfunctions

$$\begin{aligned} \phi_+(x) &= \frac{1}{\sqrt{2}} [\phi_{\text{side}}(x) + \phi_{\text{center}}(x)] \\ \phi_-(x) &= \frac{1}{\sqrt{2}} [\phi_{\text{side}}(x) - \phi_{\text{center}}(x)] \end{aligned} \tag{64}$$

(see Fig. 4). Within the WKB approximation, the gap between these levels is given by

$$\varepsilon_- - \varepsilon_+ = \frac{2}{\pi} \{[\varepsilon - V_{\text{eff}}(x_{\min})](\varepsilon - E_g)\}^{1/2} \times \exp\left\{ - \frac{(2kV_0)^{1/2}}{T_1} \int_{x_0}^{x_2} [V_{\text{eff}}(x) - \varepsilon]^{1/2}\, dx \right\} \tag{65}$$

where $x_{\min}$ is the position of one of the absolute minima of the effective potential $V_{\text{eff}}(x)$. Note that α reduces T_1 and also ε. Both of these effects reduce the gap; the lowered transition temperature is the dominant effect. This expression gives a formal result displaying the reduction of the gap ξ_2^{-1} due to the anharmonic intersite coupling. As indicated previously, this reduction of T_1 is due to the lowered vibrational entropy in the low-temperature phase when α is nonzero. Figure 10 shows that the value of the gap $\xi_2^{-1}(T_1) = (\varepsilon_- - \varepsilon_+)\, V_0/T_1$ decreases rapidly as a function of α/k, providing for the narrow finite-size-affected regime for $L_\perp = 1$. Increasing α reduces T_1, allowing for an arbitrarily small gap. Thus, by properly choosing α, one can find the 1D system arbitrarily close to a transition.

The above gap is the dominant finite-size effect, providing for the rounding in the affected regime near the transition temperature T_1. At lower temperatures the finite size of the system prevents long-range order in the system. However, this has a significantly smaller effect on the thermodynamic quantities than the rounding near T_1; this may be understood by utilizing the pseudo-Schrödinger equation. For $T \ll T_1$ the important splitting is between the ground state and the first excited state [cf. Eq. (40)]. Again, we assume that approximate wave functions may be constructed: in this case, the two wave functions are $\phi_{\text{left}}(x)$, localized in the left well, and $\phi_{\text{right}}(x) = \phi_{\text{left}}(-x)$, localized in the right well. The symmetric and antisymmetric levels are split by an amount

$$\Delta\varepsilon = \frac{\varepsilon}{\pi} \exp\left\{ -\frac{(2kV_0)^{1/2}}{T} \int_{-x_0}^{x_0} [V_{\text{eff}}(x) - \varepsilon]^{1/2}\, dx \right\} \tag{66}$$

Here, x_0 satisfies

$$\tilde{V}(x_0) = \varepsilon, \qquad 0 < x_0 < 1 \tag{67}$$

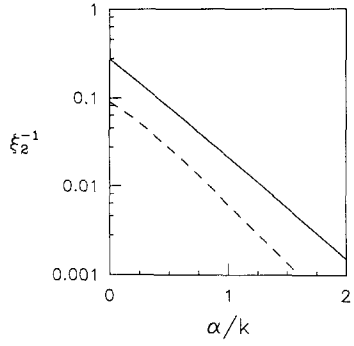

Fig. 10. Inverse correlation length ξ_2^{-1} as a function of α/k, predicted using Eq. (65) (solid line) and numerical TM results (dashed line).

The integral in the exponential in Eq. (66) may be compared to the kink energy for the $\alpha = 0$ case,[25,26]

$$E_{\text{kink}} = (2kV_0)^{1/2} \int_{-1}^{1} \tilde{V}^{1/2}(x)\, dx \tag{68}$$

The similarity between these expressions demonstrates that the gaps are indeed related to the domain walls.[25,26] The differences have been interpreted as the finite-temperature renormalization of the domain wall energy.[26,30]

We make the rough approximation

$$\Delta\varepsilon \sim \frac{\varepsilon}{\pi} \exp\left(-\frac{E_{\text{kink}}}{T_1}\right)$$

and note that $E_{\text{kink}}/T_1 \approx 15$ for our choice of parameters, to obtain an estimate for the gap at the transition:

$$\frac{\Delta\varepsilon}{\varepsilon} \lesssim 10^{-7} \tag{69}$$

This is much smaller than the gap related to ξ_2^{-1}, demonstrating that this splitting has negligible effects on the free energy. It is important to note that this small correction is the *dominant nonperturbative* correction to the ground-state energy at low temperatures, though it vanishes rapidly as $T \to 0$. Note further that choosing the parameters of the model such that the finite-size-affected regime is smaller will reduce the above estimate significantly. This demonstrates that the important corrections to the thermodynamic quantities in the harmonic approximation are due to local anharmonicities, not domain wall formation. Furthermore, as indicated in the previous sections, this low-temperature splitting decreases rapidly as a function of $L_\perp$, so that in the 2D limit the system is *completely* describable using the appropriate perturbation theory. Thus, we may expect that the free energy of the system may be calculated quite accurately by treating the anharmonicities as perturbations. Explicit calculations have demonstrated the rapid convergence of a second-order variational perturbation theory to the exact free energy.[16]

6. DISCUSSION

In this work we have shown that the exact thermodynamics of our $L_\perp \times \infty$ model undergo scaling behavior in accordance with the ansatz presented in Section 2, even for small $L_\perp$. This ansatz, a generalization of

the established ansatz appropriate for transitions with no broken symmetry, incorporates the simple idea that the finite-size scaling is controlled by the *shortest* of the diverging length scales ξ_n derived from the transfer matrix. The arguments leading to this are supported by a phenomenological form of the transfer matrix; the form presented in Section 3 for our system is appropriate for the broken $u \to -u$ symmetry, but is easily generalized. This phenomenological form allows for an analytic continuation of the free energy into the metastable regime.[14]

The scaling ansatz gives an expression for the width of the finite-size-affected regime where the rounding of the transition occurs. This, along with the identification $\xi = \exp[L_\perp \sigma(L_\perp)]$, provides for a simple understanding of the scaling behavior of our model. The rounding width is governed solely by the change of entropy at the transition (i.e., the reduced latent heat l/T_1), and by the reduced surface free energy σ associated with domains between the high- and low-temperature phases. In the case where the on-site displacement u is a continuous variable, the transition temperature is considerably lowered by anharmonic couplings which decrease the entropy of the low-temperature phase and thereby stabilizes the high-temperature phase. This decreased entropy is caused by the suppression of small-amplitude displacements about the absolute minima. By lowering the entropy of the low-temperature variants, the high-temperature phase is thermodynamically more stable, causing a lower transition temperature T_1. This increases the reduced domain wall energy $\sigma(T = T_1) = \Sigma/T_1$ significantly; the width of the finite-size-affected regime is decreased both by this and also by the increased change in entropy. The discrete version of the model lacks these small-amplitude, low-energy displacements; thus the exact calculations show that the anharmonic couplings have a less dramatic effect for this situation (cf. Tables I and II).

The model is also useful in examining how coexistence only occurs in the finite-size-affected regime. The order-parameter distribution $P(u)$ shows multiple peaks only within this regime, consistent with work studying hypercubic systems.[5] This leads to the inevitable conclusion that the incipient transition will not be detectable outside of the finite-size-affected regime for a pure system in equilibrium; this regime will be extremely small (and usually inaccessible) for experimental realizations. Within this regime, nonlinear excitations such as domain walls are present. We believe that the study of such excitations will lead to a clearer understanding of the dynamics of the transition. The absence of precursors is interesting to compare with experimental work on structural transitions: although precursors have been widely observed, careful experiments on pure, high-quality crystals show no evidence of heterophase fluctuations.[20]

Our model is ideal for the study of the dynamical properties associated

with first-order transitions, especially those in which there is no diffusion of atoms. The narrowness of the rounding regime allows for the study of the transition for systems of small $L_\perp$, which would have direct implications concerning nucleation in the full 2D systems. Also, this model is ideal for studying the finite-size effects on the decay of metastability, which is not fully understood.[31] Furthermore, the Landau-like form of Eq. (53) suggests that we could obtain a similar rapid approach to the first-order behavior though choosing an on-site potential that has *no metastable minimum*, i.e., a ϕ^6 potential with a negative second-order coefficient. We have indeed shown that this may occur in the appropriate parameter range. This will allow further studies of the dynamics of a system quenched into an unstable regime.

Although not presented here, it is useful to note that much of the equilibrium properties may be understood by a variational form of the free energy which models the system as a harmonic solid.[13,16] These results reproduce the exact free energy to within $\sim 0.1\%$, with the accuracy increasing with $L_\perp$. This strongly suggests that in the bulk limit, there will be no nonlinear excitations relevant to the bulk free energy except at the transition temperature T_1. Furthermore, even for the finite-size systems, differences between the variational free energy and the exact results are predominantly anharmonic perturbative corrections.[16]

Molecular dynamics simulations of the system have demonstrated the importance of the nonlinear excitations to the transitions; these simulations reproduce exact thermodynamic quantities shown here, and reconfirm our conclusions. For larger systems, the harmonic description is verified by the simulations both by thermodynamic results and by dynamic structure factors. Real-space analsis of trajectories show the importance of intrinsically nonlinear, nontopological "breather" excitations in the nucleation process. These results will be presented in detail elsewhere.[16]

APPENDIX. REDUCTION OF THE TI EQUATION TO A PSEUDO-SCHRÖDINGER FORM

We write the transfer-integral eigenvalue problem, Eq. (51), in the form

$$\lambda_n \phi_n(u_{i+1}) = \exp\left[-\frac{1}{2}\beta V_{os}(u_{i+1})\right] \int du_i \left(\exp\left\{-\frac{1}{2}\beta[k(u_i - u_{i+1})^2]\right\} \times \exp\left\{-\beta\left[\frac{\alpha}{4}(u_i^2 + u_{i+1}^2)(u_i - u_{i+1})^2 + \frac{1}{2}V_{os}(u_i)\right]\right\} \phi_n(u_i)\right) \tag{A.1}$$

We need to simplify the integral

$$I(x) = \int dy \exp\left[-\frac{\beta k}{2}(x-y)^2 \right] \times \exp\left[-\frac{\beta\alpha}{4}(x^2+y^2)(x-y)^2 - \frac{\beta}{2} V_{os}(y) \right] \phi(x) \tag{A.2}$$

To do this, we change variables to $z \equiv y - x$:

$$I(x) = \int dz \exp\left(-\frac{\beta k}{2} z^2 \right) f(z; x)$$
$$f(z; x) = \exp\left[-\frac{\beta\alpha}{4}(2x^2 + 2xz + z^2) z^2 - \frac{\beta}{2} V_{os}(z+x) \right] \tag{A.3}$$

Using this along with the identity

$$\int dz \exp\left(-\frac{z^2}{2t} \right) f(z) = (2\pi t)^{1/2} \left[\exp\left(\frac{t}{2} \frac{\partial^2}{\partial z^2} \right) f(z) \right]_{z=0} \tag{A.4}$$

allows us to write the transfer integral problem as

$$\left\{ \exp\left(\frac{T}{2k} \frac{\partial^2}{\partial z^2} \right) \exp\left[-\frac{\beta\alpha}{4}(2x^2 + 2xz + z^2) z^2 - \frac{\beta}{2} V_0 \tilde{V}(z+x) \right] \phi_n(z+x) \right\}_{z=0} \times \left(\frac{2\pi T}{k} \right)^{1/2} \exp\left[-\frac{1}{2} \beta V_0 \tilde{V}(x) \right] = \lambda_n \phi_n(x) \tag{A.5}$$

The left-hand side may be simplified using the operator identity

$$e^A e^B = \exp(A + B + \tfrac{1}{2}[A, B] + \tfrac{1}{6}[A, [A, B]] + \cdots) \tag{A.6}$$

We neglect terms of $\mathcal{O}(d^{-2} \equiv V_0/k)$ in the displacive limit. Furthermore, we also neglect terms of $\mathcal{O}(\alpha T/k^2)$, which is appropriate at low temperatures. With these approximations, Eq. (A.5) becomes

$$(2\pi T)^{1/2} \exp\left[-\beta V_{os}(x) + \frac{T}{2k} \frac{\partial^2}{\partial x^2} - \frac{\alpha}{4k} x^2 \right] \phi_n(x) = \lambda_n \phi_n(x) \tag{A.7}$$

Using Eq. (25), we may define the variables ε_n by

$$\lambda_n = \exp(-\beta V_0 \varepsilon_n) \tag{A.8}$$

Defining

$$V(T) = -\frac{T}{2V_0}\ln\left(\frac{2\pi T}{k}\right), \qquad \tilde{\alpha} = \frac{\alpha}{2kV_0}, \qquad m^* = kV_0\beta^2 \tag{A.9}$$

we arrive at the equation

$$\exp\left\{-\beta V_0\left[\tilde{V}(x) + V(T) - \frac{1}{2m^*}\frac{\partial^2}{\partial x^2} + \frac{1}{2}\tilde{\alpha}Tx^2\right]\right\}\phi_n(x)$$
$$= \exp(-\beta V_0\varepsilon_n)\,\phi_n(x) \tag{A.10}$$

Thus, the functions $\phi_n(x)$ satisfy the pseudo-Schrödinger equation

$$\left(-\frac{1}{2m^*}\frac{\partial^2}{\partial x^2} + \tilde{V}(x) + V(T) + \frac{1}{2}\tilde{\alpha}Tx^2\right)\phi_n(x) = \varepsilon_n\phi_n(x) \tag{A.11}$$

ACKNOWLEDGMENTS

R.J.G. thanks and acknowledges Vladimir Privman for explaining ref. 17 and Winfried Petry for discussions on his experiments showing the total absence of heterophase fluctuations. We thank Alan Bishop for motivating and discussing the pseudo-Schrödinger approach. J.R.M. acknowledges support from the DOE and partial support from the Cornell Material Science Center; and R.J.G. acknowledges support from the NSERC of Canada.

REFERENCES

1. L. Onsager, *Phys. Rev.* **65**:117 (1944).
2. M. E. Fisher, *Physics* **3**:255 (1967).
3. G. Forgacs, N. M. Švrakić, and V. Privman, *Phys. Rev. B* **37**:3818, **38**:8996 (1988).
4. M. E. Fisher and A. N. Berker, *Phys. Rev. B* **26**:2507 (1982).
5. K. Binder and D. P. Landau, *Phys. Rev. B* **30**:1477 (1984); M. S. S. Challa, D. P. Landau, and K. Binder, *Phys. Rev. B* **34**:1841 (1986).
6. V. Privman, ed., *Finite-Size Scaling and Numerical Simulation of Statistical Systems* (World Scientific, Singapore, 1990).
7. V. Privman and M. E. Fisher, *J. Stat. Phys.* **33**:385 (1983).
8. J. A. Krumhansl and R. J. Gooding, *Phys. Rev. B* **39**:3047 (1989).
9. R. J. Baxter, *J. Phys. C* **6**:L445 (1973).
10. C. J. Hamer, *J. Phys. A* **16**:3085 (1983).
11. F. Iglói and J. Sólyom, *J. Phys. C* **16**:2833 (1983).
12. R. J. Gooding, *Scripta Met.* **25**:105 (1991).
13. J. R. Morris and R. J. Gooding, *Phys. Rev. Lett.* **65**:1769 (1990); J. R. Morris and R. J. Gooding, *Phys. Rev. B* **43**:6057 (1991).

14. V. Privman and L. S. Schulman, *J. Phys. A* **15**:L231 (1982); V. Privman and L. S. Schulman, *J. Stat. Phys.* **29**:205 (1982).
15. A. D. Bruce, *Adv. Phys.* **29**:111 (1980).
16. J. R. Morris and R. J. Gooding, in preparation.
17. V. Privman and N. M. Švrakić, *J. Stat. Phys.* **54**:735 (1989).
18. E. Brézin and J. Zinn-Justin, *Nucl. Phys. B* **257**[FS14]:867 (1985).
19. H. W. J. Blöte and M. P. Nightingale, *Physica* **112A**:405 (1982).
20. W. Petry, T. Flottmann, A. Heiming, J. Trampenau, M. Alba, and G. Vogl, *Phys. Rev. Lett.* **61**:722 (1988); W. Petry, A. Heiming, J. Trampenau *et al.*, *Phys. Rev. B* **43**:10933, 10948, 10963 (1991).
21. M. P. Nightingale, In *Finite Size Scaling and Numerical Simulation of Statistical Systems*, V. Privman, ed. (World Scientific, Singapore, 1990), p. 287.
22. L. D. Landau and E. M. Lifshitz, *Statistical Physics, Part I*, 3rd ed. (Pergamon Press, 1980), p. 537.
23. N. D. Mermin and H. Wagner, *Phys. Rev. Lett.* **17**:1133 (1966).
24. D. J. Scalapino, M. Sears, and R. A. Ferrel, *Phys. Rev. B* **6**:3409 (1972).
25. J. A. Krumhansl and J. R. Schrieffer, *Phys. Rev. B* **11**:3535 (1977).
26. J. F. Currie, J. A. Krumhansl, A. R. Bishop, and S. E. Trullinger, *Phys. Rev. B* **22**:477 (1980).
27. G. F. Mazenko and P. S. Sahni, *Phys. Rev. B* **18**:6139 (1978).
28. V. Privman, *Mod. Phys. Lett. B* **5**:1031 (1991).
29. L. D. Landau and E. M. Lifshitz, *Quantum Mechanics*, 3rd ed. (Pergamon Press, 1977), p. 179.
30. A. R. Bishop, *Solid State Commun.* **30**:37 (1979).
31. L. S. Schulman, In *Finite Size Scaling and Numerical Simulation of Statistical Systems*, V. Privman, ed. (World Scientific, Singapore, 1990).